Optical excitations of poly-3-alkylthiophene films and solutions

C. Botta and S. Luzzati

Istituto di Chimica delle Macromolecole, Consiglio Nazionale delle Ricerche, via Bassini 15, I-20133 Milano, Italy

R. Tubino[*]

Istituto di Matematica e Fisica, Università di Sassari, via Vienna 2, I-07100 Sassari, Italy

A. Borghesi

Dipartimento di Fisica, Università di Modena, via Campi 213/a, I-41100 Modena, Italy

We report a comparative study of the optical properties and photoexcitations of solid-state and solution samples of poly-3-alkylthiophenes. The π-electron delocalization and backbone conformational properties are investigated by resonant and preresonant Raman scattering. Photoexcited electronic states are studied by cw photomodulation spectroscopy. The intensity and chopper-frequency dependence of the photoinduced electronic bands indicate two different photoexcitation pathways. An interchain mechanism takes place in the solid while in solution a weak solvent-polymer charge transfer is proposed.

I. INTRODUCTION

Poly-3-alkylthiophenes (PAT's) are a class of nondegenerate ground state conjugated polymers which attracted considerable attention for their processability. By proper chemical substitution in position 3 of the thiophene ring, soluble and fusible conjugated polymers are obtained which are good candidates for potential applications. Moreover, these polymers are particularly interesting because of the interaction between the electronic structure and the backbone conformation. In fact, the presence of the side chain substituent leads to thermochromic and solvatochromic effects which monitor the coupling of the electronic structure of π-electrons to the conformational changes.[1,2]

PAT's, in their solid-state form, have the same *trans* planar backbone conformation of polythiophene (PT).[3] An average conjugation length of eight C=C bonds at room temperature was estimated for poly-3-octylthiophene films.[4] In solution the chains may aggregate or stay as isolated flexible coils depending on the solvent quality. It has been well established that poly-3-hexylthiophene (PHT) exists as isolated flexible-coil chains in dilute tetrahydrofuran (THF) and chloroform solutions with a persistence length of 2.4 nm which corresponds to approximately six thiophene rings.[5] In poly-3-butylthiophene the stiffening of the chains in bad solvent has been measured by neutron scattering.[6] The persistence length, however, cannot be measured because of chain aggregation.

Resonant Raman scattering, together with optical absorption-emission spectroscopy, provides valuable information on the electronic properties of conjugated polymers and has been widely used to investigate their conjugation length.[7] In a previous work[8] we showed that in PAT's the vibrational frequency of the mode which is strongly coupled to the π-π^* transition is sensible for

"small" torsions between thiophenes rings which do not necessarily interrupt completely the conjugation path. Resonant Raman scattering is thus a fine tool to indagate the backbone conformational properties and has been used to test the quality of different PAT samples.

In conjugated polymers the strong electron-phonon coupling, typical of low dimensional systems, leads to nonlinear electronic excitations.[9] Charges added to a polymeric chain, both by doping or via photoexcitation, generate self-localized distortions of chain segments. The structure of the distorted segments depends on the presence of a preferred sense of bond alternation on the neutral chain. For polymers with degenerate ground state (polyacetylene), defects are supposed to have a metallic structure associated with segments of the chain where dimerization has been suppressed. This defect, called soliton, generates an energy level in the middle of the gap. For polymers with nondegenerate ground state (as PT and PAT), the defect has a quinoid metastable structure and it can be viewed as formed by two bound solitons which generate two levels in the gap. For this second family of polymers, charged nonlinear electronic states are polarons ($\pm e$) and bipolarons ($\pm 2e$), with spin $\frac{1}{2}$ and 0, respectively. Photogeneration of these charged defects requires separation of electrons and holes into different chains in order to prevent geminate recombination. Thus polarons and bipolarons are metastable states generated via an interchain hopping process. Bipolarons (BP's) are obtained by the coalescence of two polarons with the same charge according to an equilibrium reaction:

$$P^+ + P^+ \rightleftharpoons BP^{2+} , \qquad (1)$$

where the bipolaron is energetically favored because it minimizes the extension of the quinoid segment of the chain with respect to two polarons, while polarons are favored by the entropic term associated with their spin. The primary species generated via photoexcitation are

neutral nonlinear states resulting from an intrachain electron-hole separation. These states are called neutral bipolaron or polaron-exciton and decay radiatively if generated in the singlet state. Triplet metastable states have also been reported for polydiacetylenes[10] and polyphenilenevinilene.[11] Photoinduced absorption (PA) in the visible and near-infrared region (NIR) by a cw modulation technique is widely used to detect energy states in the gap associated with long-lived photogenerated nonlinear electronic states. Light induced electron spin resonance (LESR) or optically detected magnetic resonance (ODMR) are used to indagate their magnetic properties.[12]

PAT's represent a good model system for studying photoexcitations because in these polymers interchain interactions can be drastically varied by changing the supermolecular organization of the samples. Bipolaronic states were observed in solid-state samples of PHT by photoexcitation and by chemical doping.[13,14] With respect to chemical doping, photoinjection of electrons and holes by PA offers the advantage of adding charges without the presence of counterions. Counterions generally stabilize bipolarons over polarons by screening the electron-electron Coulomb repulsion. PA experiments have not showed evidence for polarons in PAT solid-state samples although assignment of some bands is still not clear. A tentative assignment to triplet exciton in poly-3-dodecylthiophene[14] seems to be supported by ODMR results.[15] By charge injection in semiconductor device structures both bipolarons and polarons were observed.[16] This technique allows us to control the concentration of injected charges, thus obtaining thermodynamic equilibrium conditions at which polarons can be detected.

Chemical doping PHT solutions has been performed for different solvent polarities and both polarons and bipolarons were detected.[17] In particular, polarons could be observed at low concentration of dopants only in polar solvents (CH_2Cl_2) while in less polar solvents such as $CHCl_3$ a small concentration of polarons can exist only for high polymer concentrations. This behavior is explained as a reduction in the screening effect of the counterion obtained either by a polar solvent or by a high concentration of doped polymer. The consequent enhancement of the electron-electron repulsion can thus allow a dominant equilibrium population of polarons over the bound energetically favored bipolarons. PA measurements have been performed on solutions of PHT (Ref. 18) and poly-3-decylthiophene.[19]

The aim of the present work is to understand the role of the interchain charge separation on the photoexcitation pathway. To this purpose we have extensively studied, using optical, Raman, and photomodulation spectroscopy, samples of PAT of different supermolecular organization such as films, "good" and "bad" solvent solutions. Our results indicate the presence of two quite different photoexcitation mechanisms. One, taking place in the solid phase, requires charge separation onto two different chains of the photogenerated pair. Bipolarons are then formed by a bi-molecular mechanism when two chargelike polarons coalesce on the same chain. The other mechanism takes place in solution where interchain charge separation cannot occur. In this case certain solvents can form charge transfer complexes with the photoexcited polymer thus producing a photoinduced doping which leads to polarons and/or bipolarons. As will be discussed, these two photoexcitation mechanisms are detected through a marked difference of the intensity and chopper-frequency dependence of the photoinduced signal.

II. EXPERIMENT

Poly-3-decylthiophene (C10) was chemically synthesized as described in Ref. 20. The characterization of C10 has been performed by NMR, indicating a concentration of head to head defects of 1:12. The molecular weight determined by gel permeation (GP) chromathography is $M_w = 12\,700, M_w/M_n = 1.86$ which corresponds to 57 rings. The chain overlap concentration c^* is estimated to be higher than 2×10^{-2} g/ml, on the basis of an extensive characterization of PHT solutions.[5] X-ray diffraction results are reported elsewhere.[3]

Absorption spectra are recorded with a Cary 2400 spectrophotometer. Raman spectra are obtained with excitation in the visible region using an Ar^+ and an He-Ne laser. The power impinging the sample is about 1 mW and samples are kept under nitrogen atmosphere. We have used a flat field Jasco TRS300 polychromator with a 512 intensified diode array (EG&G 1420) interfaced to a XT286 IBM PC by an EG&G 1461 microprocessor. In the NIR region the Raman spectra have been performed with a Bruker Fourier transformer spectrometer (IFS66+FA106), working with a Nd-YAG laser (1064 nm) (where YAG denotes aluminum yttrium garnet) with a power emission kept lower than 150 mW. Measurements on solid C10 samples have been performed on cast films from $CHCl_3$ solution.

PA measurements have been performed using a mechanically chopped cw Ar^+ laser as the pump and a tungsten halogen lamp as the probe. Optical transmission, dispersed with a grating monochromator, is measured in the visible and near-infrared region with a photomultiplier tube and a cooled PbS detector. Measurements have been performed under vacuum on C10 cast films on quartz substrates both at room temperature and at 80 K. The PA spectrum of C10 solutions, prepared with dry solvents in a free oxygen quartz cell, are obtained at room temperature with a 514-, 488-, and 457.9-nm pump beam. The samples have been prepared as (i) cast films from chloroform solution: C10-FLM and C10a-FLM (the latter has been obtained upon dissolution of the C10 polymer where a few impurities have been introduced by a previous thermal treatment in air atmosphere); (ii) chloroform (C10-CLF), benzene, toluene, and carbon tetrachloride good solvent solutions. The solutions are at diluted concentration $c \sim 10^{-3}$ g/ml ($c \ll c^*$) so that chains in the good solvent solutions are not aggregated. The absence of aggregates has been directly checked for C10-CLF by quasielastic light scattering. This is consistent with the results of recent study by Heffner and Pearson,[5] who have concluded that in chloroform PAT "exists as nonaggregated flexible-coil
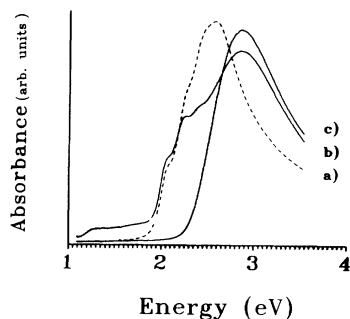
FIG. 1. Optical absorption spectra of C10 measured at room temperature: (a) C10-FLM, (b) C10-CMP, and (c) C10-CLF.

TABLE I. Raman modes of poly-3-hexylthiophene (C7), in cm^{-1}, for 454.52-nm excitation wavelength at 80 K (vs=very strong, s=strong, m=medium, w=weak, vw=very weak). Fundamental (f) and overtone (o) modes are measured with 4- and 8-cm^{-1} resolution, respectively.

f	f	o (observed)	o (calculated)
599 w	1022 vw	2186 w $\mu_6+\mu_1$	2191
680 w	1092 m μ_3	2474 w $\mu_6+\mu_2$	2474
727 m μ_1	1169 m	2566 w $\mu_6+\mu_3$	2556
740 w	1199 m μ_4	2660 m $\mu_6+\mu_4$	2663
831 vw	1219 w	2840 m $\mu_6+\mu_5$	2848
884 vw	1384 s μ_5	2928 s $2\mu_6$	2928
995 w	1464 vs μ_6		
1010 w μ_2	1522 m		

molecules." (iii) 2-chlor-2-methyl-propane (C10-CMP) and benzonitrile (C10-BN) bad solvent solutions.

III. RESULTS

A. Optical absorption

In Fig. 1 are shown the absorption spectra of C10 samples. Curve a represents the solution cast film C10-FLM whose spectrum is similar to C10a-FLM. Curve b shows the poor solvent solution C10-CMP, whose spectrum is similar to C10-BN, while curve c shows the spectrum of the good solvent solution C10-CLF, whose spectrum is similar to the other good solvent solutions. The vibronic structure of the solid sample is related to the ordered crystalline phase. The loss of backbone planarity upon dissolution shifts the absorption maximum from 2.43 to 2.86 eV (see curves a and c). Curve b is characteristic of a two-phase solution: a completely solvated phase and an aggregated one, in agreement with a previous study of mixed solvent system for PHT.[1] The aggregated phase of the bad solvent solutions increases after some days from the preparation and then reaches an equilibrium condition.

B. Resonant Raman scattering

Figure 2 shows the Raman spectrum of a PAT cast film obtained at 80 K with the 454.52-nm exciting wavelength. The peak frequencies are listed in Table I where we have labeled by μ_i the modes which give overtones and combinations (A_g modes). Raman features are simi-

lar to poly-3-methylthiophene,[21] while the number of vibrational modes is much higher than in PT. The band frequencies do not depend on the alkylic chain length, being the same for C7, C10, and C11.[8] Moreover, they do not shift with the exciting wavelength with the exception of μ_6, which is the backbone mode mostly coupled to the electronic transition containing an important contribution of C=C stretching.[8] This assignment agrees with that recently reported for polyoctylthiophene,[4] while, from effective conjugation coordinate calculations, assignment to a ring vibration in which the sulfur atom is strongly involved has been suggested.[22] μ_6 shows a dispersion with the exciting wavelength which is sample dependent and it is coherently related to the distribution of conjugation lengths as monitored by the absorption spectra.[8] This dispersion is plotted in Fig. 3 for several PAT samples. It is known that in PT (Ref. 23) the C=C stretching frequency is not sensitive to the conjugation length because for oligomers longer than trimers it converges to the value of the polymeric chains. The different behavior of PAT's can be accounted for by the wider distribution of effective conjugation lengths present in the substituted polymer. Our results are not in contrast with a mean conjugation length of four monomers proposed
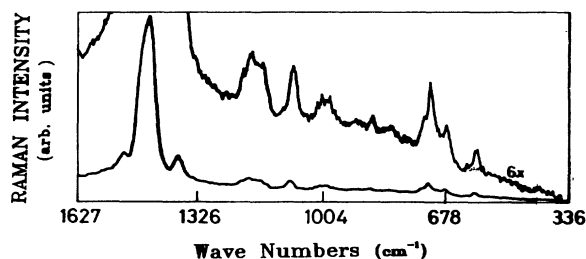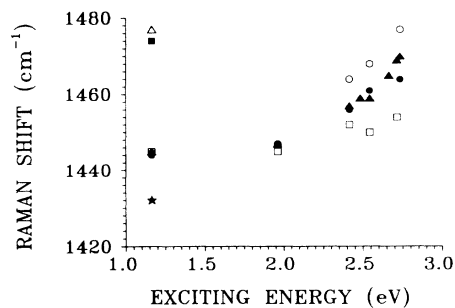

FIG. 2. Raman spectrum of a chemically synthesized poly-3-heptylthiophene (C7) cast film recorded at 80 K with 454.52-nm exciting wavelength.

FIG. 3. Frequency dispersion of the μ_6 Raman mode. C7 (solid circle) and C10 (open square) chemically synthesized cast films. Electochemically synthesized films of polyheptylthiophene (open circle), and polyundecylthiophene C11 (solid triangle). C7 chloroform solution (solid square), C10-CLF (open triangle), and C10-CMP (solid star).
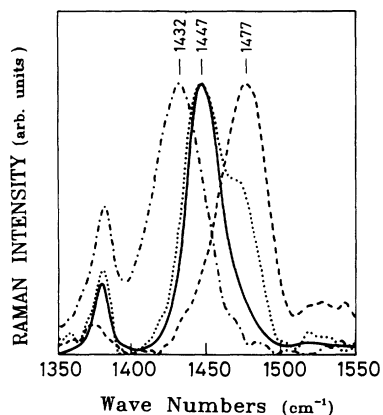
FIG. 4. Raman spectra of C10-CMP (dashed-dotted line), C10-BN (dotted line), C10-FLM (solid line), and C10-CLR (dashed line) recorded at $T=300$ K with 1064-nm exciting wavelength.

by Danno, Kurti, and Kuzmany.[4] From Fig. 3 it can be seen that C10 is quite an ordered polymer with a large mean conjugation length and a narrow distribution.

Raman spectra of the solutions have been measured by exciting in the NIR region because the samples are strongly luminescent in the visible region. The spectral features do not vary upon dissolution with the exception of a shift of the μ_6 band to higher frequencies. These changes are depicted in Fig. 4, where the spectra of the C10 solid sample and solutions are plotted. The μ_6 band shifts from 1477 cm^{-1} (good solvent solutions) to 1447 cm^{-1} (cast film) displaying a shift of 30 cm^{-1} upon dissolution in a good solvent. The bad solvent solution in benzonitrile shows two components: the good solvent and the cast film band. These are related to the dissolved and the aggregated phase. In CMP the band of the dissolved phase is only a small feature possibly because the weight of the aggregated phase is resonantly enhanced by some absorption at low energy (see Fig. 1). For this reason the longer conjugation lengths are selectively enhanced, thus explaining a Raman shift lower than in the solid.
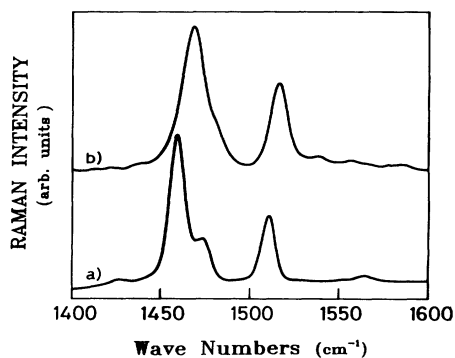
Our results indicate that the C$=$C stretching frequen-

cy changes upon dissolution are coherently related to the reduction of the conjugation length. Alkyl side chains in fact introduce an entropic term responsible for interring torsions in the thiophene backbone, which can account for thermochromic and solvatochromic transitions.[22] To prove the role of backbone rotations in the μ_6 frequency dispersion we have measured the Raman spectra of the pentathiophene oligomer (T5) both in solid state and in solution. The 1459-cm^{-1} C$=$C stretching frequency of T5 in the solid state shifts upwards to 1468 cm^{-1} upon dissolution in chloroform, as shown in Fig. 5. The C$=$C stretching vibrational frequency is thus affected by a loss of backbone planarity at a short-range scale (less than three monomers).

C. Photoluminescence

Photoluminescence (PL) of C10 solid samples is peaked at 1.8 eV and shows three well-resolved vibronic peaks where energy spacing (0.18 eV) is comparable to the separation of the shoulders of the absorption spectra and corresponds to the C$=$C Raman stretching frequency. For C10 cast films the energy position of the PL band does not show any dependence on exciting energy, while we find a strong dependence for electropolymerized films, reflecting their wider conjugation length distribution.[24] C10 solutions have a PL maximum at 2.18 eV with the same Stokes shift (0.66 eV) of solid samples. PL quantum yield is much higher in solution than in the solid phase and it is higher in the good solvent solutions with respect to the bad solvent ones thus decreasing with solvent polarity. Moreover, PL bands do not change in shape and position for different solvents, indicating that in PAT samples the most disordered phase is the main source of PL.[25]

D. Photoinduced absorption

The absorption-emission properties, the relatively narrow distribution of conjugation lengths, as observed from the dispersion of the C$=$C stretching vibration in C10 samples (see Fig. 3), lead us to conclude that C10 provides a good system for studying the properties of the photoexcited states in PAT's. Moreover, from their optical characterization, we can assert that samples with three different supermolecular organizations are available: solid-state samples (C10-FLM and C10a-FLM) where the ordered phase has trans planar backbone conformation; good solvent dilute solutions (C10-CLF,C10 in benzene, toluene, and carbon tetrachloride) where chains exist as isolated flexible coils affected by a loss of backbone planarity due to interring rotations; bad solvent solutions (C10-CMP and C10-BN) with an aggregated and dissolved phase where the chain conformation is similar to that of the solid sample and of the good solvent, respectively.

1. Solid samples

The PA spectrum of C10 solution cast film (C10-FLM) can be measured even at room temperature (see Fig. 6). The spectral features are similar to PHT solid sam-
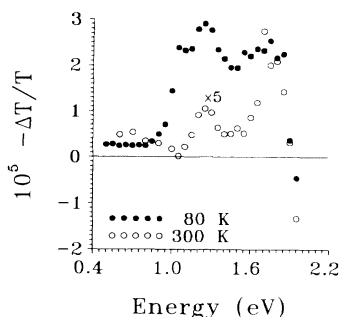

FIG. 5. Raman spectra of T5 both in the solid state (curve a), and in CHCl$_3$ solution (curve b) recorded at room temperature with 1064-nm exciting wavelength.

FIG. 6. Photoinduced absorption spectra of C10-FLM obtained with a 488-nm pump beam (100 mW/cm^2) chopped at 85 Hz, at room temperature, and at $T = 80$ K.

FIG. 8. Chopper frequency dependence of the photoinduced signal of C10a-FLM at 0.4 eV, measured with a 488-nm pump beam (90 mW/cm^2) at $T = 80$ K.

ples.[13,14] In the high-energy region, two bands, which are the signature of photoinduced states, are seen at 1.25 and 1.75 eV. $\Delta T/T$ increases upon cooling while the relative intensity of the 1.75-eV band decreases with temperature; at 80 K the two peaks reach the same height. The relative intensity is, however, sample dependent; Fig. 7 shows a PA spectrum obtained at 80 K for frequencies between 0.3 and 2 eV for the (C10a-FLM) sample. The spectrum exhibits three broadbands at 1.75 eV, 1.25 eV, and at energy ≤ 0.35 eV. The 1.75 component is quite intense showing that this band is affected both by conformational and chemical defects. Moreover, we have found that the 1.75-eV phase lag is higher with respect to the 1.25-eV band. This implies that the lifetimes are longer in the high-energy component.

Figure 8 shows the chopper frequency dependence of the photoinduced signal of C10a-FLM at 0.4 eV. At 1.2 eV the frequency response is very similar, indicating that these two bands have the same origin while a slightly different behavior is observed at 1.75 eV. The signal decreases as $\omega^{-1/2}$ for frequencies higher than 100 Hz and the response is still rising at low frequencies, even at 2 Hz, indicating the presence of a lifetime distribution with components higher than 0.5 sec.

The photoinduced signal increases with pump intensity (see Fig. 9) according to a $I^{0.6}$ law for the three bands independently from the chopper frequency. This is the evi-
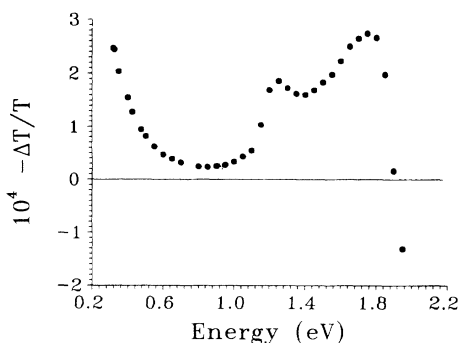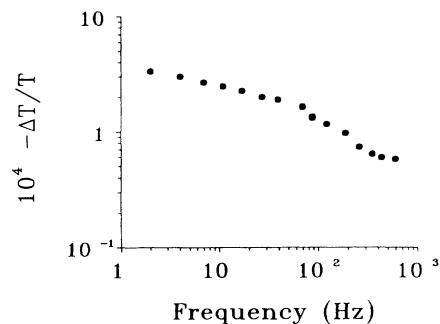
dence that the photoexcited species are created and recombine via a bimolecular process, thus indicating the formation of charged excitations.

The existence of two different kinds of bipolarons was claimed for PHT (Ref. 13) and may also explain our data. The 1.25- and 0.35-eV transitions are assigned to bipolarons whose signature is found in the PA spectra of several thiophene based polymers. The second kind, which is peculiar of poly-3-decylthiophene and of PHT, possibly corresponds to long-lived trapped bipolarons whose concentration varies with the number of conformational and chemical defects. These combined bipolarons are identified by the 1.75-eV transition and, in analogy to PHT, by a low-energy transition around 0.2 eV. This latter band cannot be detected with our experimental setup. This assignment is, however, not consistent with the results quoted in Ref. 26, where the band at 1.75 eV has a shorter lifetime than that of the two lower-energy peaks. Moreover, this band falls into a spectral region possibly complicated by the absorption of polarons.

2. Solutions

The PA spectrum obtained at room temperature on a chloroform solution (C10-CLR) at $c = 1 \times 10^{-3}$ g/ml is shown in Fig. 10. Three subgap electronic transitions are

FIG. 7. Photoinduced absorption of C10a-FLM obtained with a 488-nm pump beam (80 mW/cm^2) chopped at 17 Hz, at $T = 80$ K.
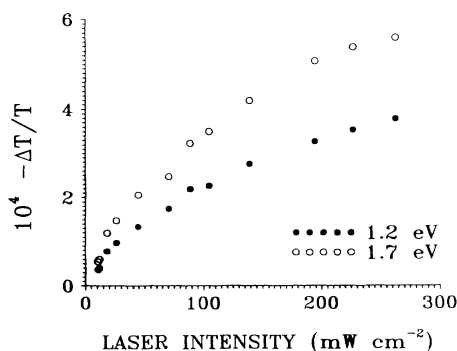

FIG. 9. Laser intensity dependence of the photoinduced peaks of C10a-FLM at 1.7 eV (open circle) and 1.2 eV (solid circle), measured with a 488-nm pump beam chopped at 17 Hz, at $T = 80$ K.
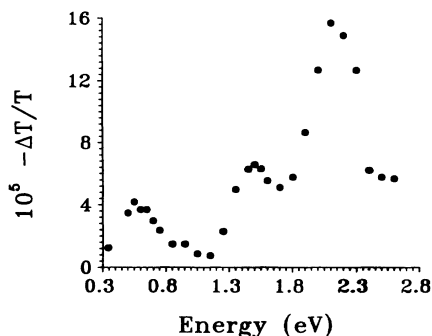
FIG. 10. Photoinduced absorption of C10-CLR obtained with a 457.9-nm pump beam (80 mW/cm^2) chopped at 23 Hz, at room temperature.

FIG. 12. Photoinduced absorption of C10-CMP obtained with a 514.52-nm pump beam (80 mW/cm^2) chopped at 23 Hz, at room temperature.

visible at 0.55, 1.55, and 2.1 eV. Interchain charge hopping does not appear to play any role in the photoexcitation pathway for the following reasons: (i) there is no evidence of aggregation in chloroform solutions as reported in a previous section; (ii) the very same PA transitions have been observed for a very dilute solution at $c = 4 \times 10^{-4}$ g/ml, thus well below the overlap concentration c^*.

Figure 11 shows the PA spectrum of C10-BN solution at room temperature. This bad solvent solution exhibits spectral features which are different both from the solid and from the good solvent solutions. The three bands of the chloroform solution are observed in addition to a very intense band at 1.75 eV. The other bad solvent solution C10-CMP shows a similar PA spectrum but the intensity of the 1.75-eV band is drastically reduced and is comparable to the intensity of the 0.55- and 1.55-eV transitions (see Fig. 12).

The optical absorption spectra and Raman results previously discussed indicate that C10-BN and C10-CMP contain both an aggregated and dissolved phase. The three bands in common with the chloroform solutions may be associated with the dissolved phase.

The 1.75-eV band arises from the aggregated chains and is related to long-lived trapped photoexcited species, probably the same confined bipolarons of the solid samples. This assertion is based on the following experimen-
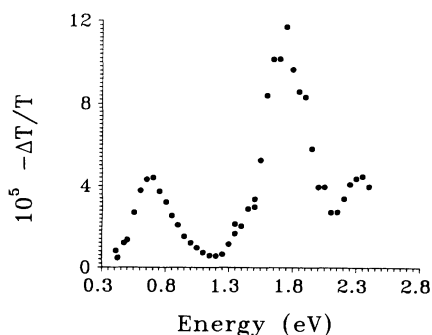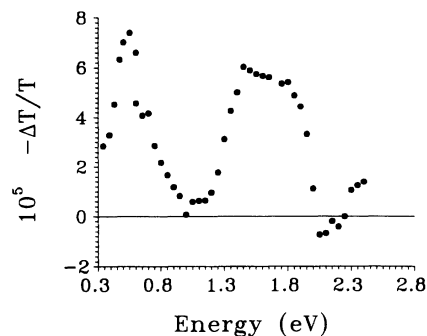
tal evidence: (i) In C10-BN solutions the phase lag of the 1.75-eV band is different from the phase of the 0.62- and 1.6-eV transitions. (ii) The 1.75-eV peak is only found in solutions with aggregated chains and in solid samples. (iii) Similar to the solid the intensity of the 1.75-eV band depends on the concentration of impurities. In fact, the extent of the aggregated chains seems less important in C10-BN solutions than in C10-CMP but a slight photooxidation occurred in the C10-BN sample.

The frequency and intensity dependence of the photoinduced signal at 0.55 and 1.55 eV have been studied for the C10-CMP solutions (see Figs. 13 and 14). The behavior of these two bands, associated with the dissolved phase, is very different from that observed in the solid samples. We prefer not to consider the 2.2-eV band because the measurements in a region so close to the band gap may be affected by electromodulation phenomena or by experimental factors as a bad subtraction of the luminescence. The signal decreases with the frequency as $\omega^{-0.7}, \omega^{-0.8}$ in the whole range studied (2–120 Hz) indicating that the lifetimes are longer in solution than in the solid sample. The intensity can be fitted by a $I^{0.94}$ law for the two bands. The observed behavior is consistent to a "single chain" mechanism for the photoexcitations as will be discussed in the next paragraph.

In order to clarify the origin of the photoexcited states observed in the solutions, we have performed additional measurements using several solvents. It can be seen from
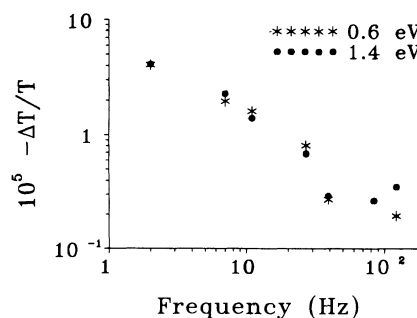
FIG. 11. Photoinduced absorption of C10-BN obtained with a 488-nm pump beam (80 mW/cm^2) chopped at 23 Hz, at room temperature.

FIG. 13. Chopper frequency dependence of the photoinduced peaks of C10-CMP at 0.6 and 1.4 eV, measured with a 514.52-nm pump beam (80 mW/cm^2) at room temperature.
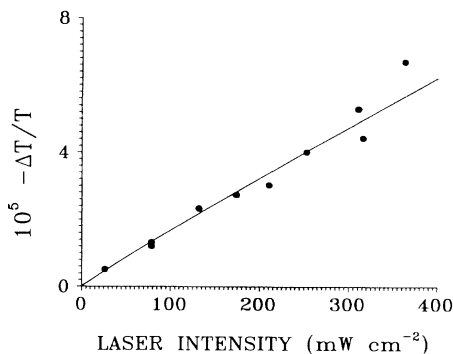
FIG. 14. Intensity dependence of the photoinduced signal of C10-CMP at 0.6 eV, measured with a 514.52-nm pump beam chopped at 23 Hz, at room temperature.

the results summarized in Table II that the energy position of the low-energy PA peak is coherently related to the energy gap of the dissolved phase of the solutions. Both CCl_4 and benzonitrile solutions displayed a photo-degradation which shifts the absorption maximum and the PA peak position to higher energies. Moreover, PA response in PAT solutions does not depend on chain aggregations: two bad solvent [C_6H_5CN, $(CH_3)_3CCl$] and two good solvent ($CHCl_3$,CCl_4) solution show PA activity.

IV. PHOTOEXCITATION MECHANISM IN SOLUTION AND IN SOLID PHASES

The experimental data on samples of various supermolecular organization reported in the preceding sections, indicate that while photoinduced absorption is always detected in the solid samples, this effect in solution is observed only in a few solvents (see Table II). It is quite apparent that the photoinduced activity does not depend on the solvent dielectric constant or on the extent of aggregation in solution. This rules out the possibility that PA bands observed in solution are related to bipolarons created by coalescence of two polarons through an interchain hopping mechanism.

The intensity and the chopper-frequency dependence of the PA bands changes in going from the solid ($\Delta T/T \sim I^{0.6}$;$\Delta T/T \sim \omega^{-1/2}$); to the solution ($\Delta T/T \sim I$;$\Delta T/T \sim \omega^{-0.8}$). This observation combined with

TABLE II. Absorption maximum positions of C10 solutions; position and $\Delta T/T$ maximum intensity of the low-energy PA peak for samples of the same optical density. The dielectric constant ϵ and the dipole moment μ of the solvents are taken from Ref. 27.

Solvent	Abs. max. position (eV)	PA peak position (eV)	$-\Delta T/T$ (arb. units)	ϵ	μ
$CHCl_3$	2.86	0.52	1	4.81	1.15
C_6H_5CN	2.97	0.6	1.7	25.2	4.05
$(CH_3)_3CCl$	2.86	0.52	2.4	9.96	2.15
CCl_4	2.86–3.29	0.73–0.8	1–0.1	2.24	0
C_6H_6	2.84		0.01	2.27	0
$C_6H_5CH_3$	2.93		0.06	2.38	0.31

the fact that PA activity is observed only in selected solvents suggests a different photoexcitation mechanism for the solid and solution. In the following section we propose a possible photoexcitation scenario for both films and solutions. The model for the films has been already reported by several authors and is included here for completeness. On the other hand, the model for the solutions is only speculative but provides a possible interpretative scheme for the present experimental results.

A. Films and aggregated phases

In solid samples or when aggregation is present, it is usually assumed that, under cw detection, charge is predominantly stored in spinless bipolarons formed through bimolecular recombination of two equally charged polarons located on the same chain (via interchain hopping). Assuming that their decay takes place through collision between oppositely charged species, the rate equation

$$\frac{dn_P}{dt} = gI - B_P n_P^2 , \qquad (2)$$

$$\frac{dn_{BP}}{dt} = B_P n_P^2 - B_{BP} n_{BP}^2 , \qquad (3)$$

implies that the concentration n of the charged excitations scales with the square root of the laser intensity as experimentally observed in solid samples. g is the generation term, and B is the bimolecular recombination constant.

B. Solutions

It is possible that a charge transfer between the solvent and the photoexcited polymer takes place. This process depends on the electron affinities E_A of the polymer and the solvent. The direct measurements of the E_A have been in most cases carried out in gas phase and cannot be used in the present context. The E_A can be evaluated by the relation

$$E_A \sim I_P - E_g + \delta , \qquad (4)$$

where I_P is the ionization potential, E_g is the energy of the highest occupied molecular-orbital to the lowest unoccupied molecular-orbital optical transition and δ is the electronic correlation term which, for a rough estimate, can be neglected. This yields $E_A = \sim 3$ eV for PAT,[28] $E_A = \sim 4.34$ eV for $CHCl_3$,$E_A = \sim 4.17$ eV for C_6H_5CN, $E_A = \sim 3.13$ eV for C_6H_6, and $E_A = \sim 2.8$ eV for $C_6H_5CH_3$, which indicates that a net energy gain occurs upon transfer of one electron from the polymer to C_6H_5CN and to $CHCl_3$, but not to C_6H_6 and $C_6H_5CH_3$ which have the lowest electron affinities.

When the electron transfer takes place a net charge on the polymer backbone is left (photoinduced doping). Because of the strong electron-phonon interaction, this excess charge is self-trapped in the lattice in a polaron state. Two possibilities can occur at this point:

(i) The polaron is annihilated through the interaction with the solvent, leaving an e-h pair on the polymer
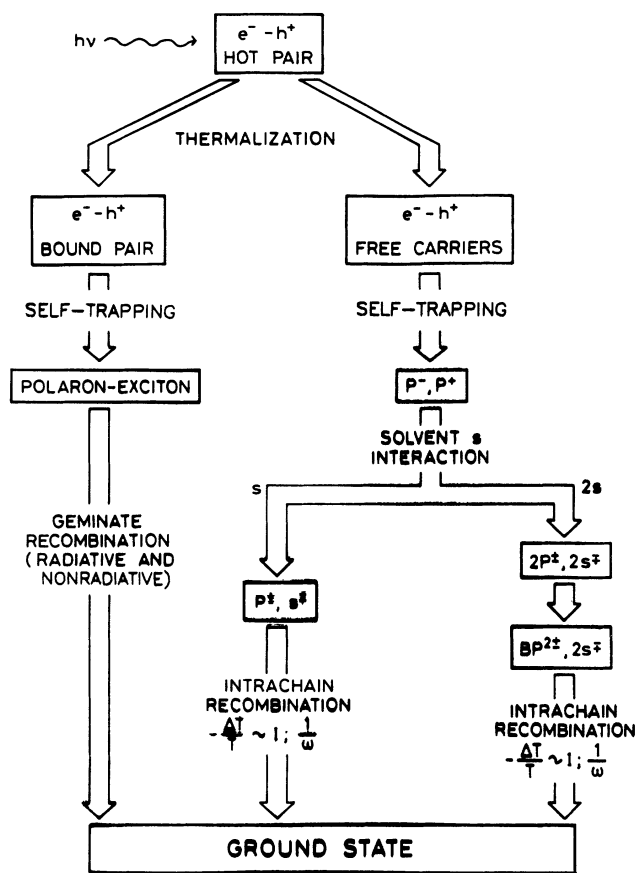
FIG. 15. Scheme of the solvent mediated intrachain generation, and recombination of photoexcitations in PAT solutions.

which recombine with radiative emission. This might well be the preferred decay mechanism as it is likely that these polarons are metastable. In fact, at dilute concentration and in low molecular weight samples polaron mobility is restricted thus inhibiting bipolaron formation. The rate equation in this case is

$$\frac{dn_P}{dt} = gI - M_P n_P , \qquad (5)$$

M_P being the recombination constant for the polaron through charge transfer with the solvent ($M_P = 1/\tau_P$ if charge migration does not take place in the solvent). Under cw conditions this equation implies a linear dependence of the polaron concentration upon laser intensity.

(ii) If polaron mobility and concentration are high enough, two polarons can collide giving rise to a bipolaron. Again, a bipolaron can decay through interaction with two charged solvent molecules corresponding to the rate equation

$$\frac{dn_P}{dt} = gI - B_P n_P^2 , \qquad (6)$$

$$\frac{dn_{BP}}{dt} = B_P n_P^2 - M_{BP} n_{BP} , \qquad (7)$$

where M_{BP} is the recombination constants of the bipolarons. In the steady-state conditions limit, also the bipola-

ron concentration n_{BP} depends linearly on the laser intensity. All in all the proposed model predicts a linear dependence of the PA bands (either polarons or bipolarons) on I as indeed observed. The existence of either polarons or bipolarons as the dominant charged excitations in solution will then depend on the experimental condition such as excitation density, solvent polarity, temperature, polymer concentration, as it has been demonstrated in a study on the solution doping.[17]

It is interesting to notice that $\Delta T/T$ of PHT in CH_2Cl_2 has been found to be, in highly absorbing samples, independent of the polymer concentration c.[18] The dependence of $\Delta T/T$ on c gives, similarly to the I and ω dependence, some insight into the photoexcitation mechanism. This can be understood by the following: (a) The generation term g is proportional to the absorption coefficient of the pump $\alpha_p = \epsilon c$. (b) The fractional transmission change $\Delta T/T$ is related to the PA coefficient $\Delta \alpha$ by the relation

$$\frac{\Delta T}{T} = l \Delta \alpha , \qquad (8)$$

where $\Delta \alpha$ is proportional to the number of the photoexcited states and l is the laser penetration depth $l = 1/\alpha_p$ for highly absorbing samples ($1/\alpha_p < \Delta x, \Delta x$ sample thickness) or $l = \Delta x$ for weakly absorbing samples. For a monomolecular mechanism, as that proposed for the solutions, for highly absorbing samples $\Delta T/T$ is predicted to be independent of c. For a bimolecular recombination mechanism, as proposed for the solid, $\Delta T/T$ should scale as $c^{1/2}$ for highly absorbing samples.

Photoexcitation pathway for the solution can be depicted by the scheme of Fig. 15. Although the triplet exciton could also account for the observed intensity and chopper-frequency dependence, the proposed model of photoinduced doping of PAT solutions explains also why (i) the position of the PA bands in solution is identical to the position of the doping induced bands; (ii) the PA is observed only in selected solvents; (iii) PA intensity in solution is essentially independent of the concentration.

V. CONCLUSIONS

By an extensive study by optical, Raman, and photomodulation spectroscopy of samples of PAT exhibiting different supermolecular organizations (solid films, aggregated solutions, "good solvent" solutions) we have been able to recognize PA peaks associated with the dissolved phase and the aggregated phase. For the dissolved phase a mechanism of photoinduced doping by the solvent is proposed to account for the main experimental features of the photoexcitation spectra in this phase. This mechanism, which, depending on the experimental conditions, can lead to the formation of polarons and/or bipolarons as the main charge storage configurations, do not require charge separation on different chains.

ACKNOWLEDGMENTS

*Also at Istituto di Chimica delle Macromolecole, Consiglio Nazionale delle Ricerche, via Bassini 15, I-20133 Milano, Italy.

[1]S. D. D. V. Rughooputh, S. Hotta, A. J. Heeger, and F. Wudl, J. Polym. Sci. Polym. Phys. **25**, 1071 (1987); B. Themans, W. R. Salaneck, and J. L. Bredas, Synth. Met. **28**, C359 (1989).

[2]O. Inganas, W. R. Salaneck, J. E. Osterholm, and J. Laakso, Synth. Met. **22**, 395 (1988); W. R. Salaneck, O. Inganas, J. O. Nilsson, J. E. Osterholm, B. Themans, and J. L. Bredas, *ibid.* **28**, C451 (1989).

[3]A. Bolognesi, M. Catellani, S. Destri, and W. Porzio, Makromol. Chem. Rapid Commun. **12**, 9 (1991).

[4]T. Danno, J. Kurti, and H. Kuzmany, Phys. Rev. B **43**, 4809 (1991).

[5]G. W. Heffner and D. S. Pearson, Macromol. **24**, 6295 (1991).

[6]J. P. Aime, F. Bargain, M. Schott, H. Eckhardt, G. G. Miller, and R. L. Elsenbaumer, Phys. Rev. Lett. **62**, 55 (1989).

[7]D. B. Fitchen, Mol. Cryst. Liq. Cryst. **83**, 1127 (1982).

[8]C. Botta, S. Luzzati, A. Bolognesi, M. Catellani, S. Destri, and R. Tubino, in *Advanced Organic Solid State Materials,* edited by L. Y. Chiang, P. M. Chaikin, and D. O. Covan, MRS Symposia Proceedings No. 173 (Materials Research Society, Pittsburgh, 1990), p. 397.

[9]A. J. Heeger, S. Kivelson, J. R. Schrieffer, and W. P. Su, Rev. Mod. Phys. **60**, 781 (1988).

[10]L. Robins, J. Orestein, and R. Superfine, Phys. Rev. Lett. **56**, 1850 (1986).

[11]N. F. Colaneri, D. D. C. Bradley, R. H. Friend, P. L. Burn, A. B. Holmes, and C. W. Spangler, Phys. Rev. B **42**, 11 670 (1990); L. S. Swanson, P. A. Lane, J. Shinar, and F. Wudl, *ibid.* **44**, 10 617 (1991).

[12]Z. Vardeny, E. Ehrenfreund, J. Shinar, and F. Wudl, Phys. Rev. B **35**, 2498 (1987).

[13]Y. H. Kim, D. Spiegel, S. Hotta, and A. J. Heeger, Phys. Rev.

B **38**, 5490 (1988).

[14]J. Rhue, N. F. Colaneri, D. D. C. Bradeley, R. H. Friend, and G. Wegner, J. Phys. Condens. Matter **2**, 5465 (1990).

[15]L. S. Swanson, J. Shinar, and K. Yoshino, Phys. Rev. Lett. **65**, 1140 (1990).

[16]K. E. Ziemelis, A. T. Hussain, D. D. C. Bradley, R. H. Friend, J. Rhue, and G. Wegner, Phys. Rev. Lett. **66**, 2231 (1991).

[17]M. J. Nowak, D. Spiegel, S. Hotta, A. J. Heeger, and P. A. Pincus, Macromolecules **22**, 2917 (1989).

[18]D. Spiegel, P. Pincus, and A. J. Heeger, Synth. Met. **28**, C385 (1989).

[19]C. Botta, A. Bolognesi, S. Luzzati, R. Tubino, and A. Borghesi, Synth. Met. **41-43**, 1323 (1990).

[20]W. Porzio, A. Bolognesi, S. Destri, M. Catellani, and G. Bajo, Synth. Met. **41**, 537 (1990); P. Stein, A. Bolognesi, M. Catellani, S. Destri, and L. Zetta, *ibid.* **41**, 559 (1990).

[21]E. F. Steigmeier, H. Auderset, W. Kobel, and D. Baeryswyl, Synth. Met. **18**, 219 (1987).

[22]G. Zerbi, B. Chierichetti, and O. Inganas, J. Chem. Phys. **94**, 4637 (1991); G. Zerbi, B. Chierichetti, and O. Inganas, *ibid.* **94**, 4646 (1991).

[23]Y. Furukawa, M. Akimoto, and I. Harada, Synth. Met. **18**, 151 (1987); M. Akimoto, Y. Furukawa, H. Takeuchi, I. Harada, Y. Soma, and M. Soma, *ibid.* **15**, 353 (1986).

[24]K. Yoshino, Y. Manada, M. Onoda, and R. Sugimoto, Solid State Commun. **70**, 111 (1989).

[25]J. R. Linton, C. W. Frank, and S. D. D. V. Rughooputh, Synth. Met. **28**, C393 (1989).

[26]G. S. Kanner, Ph.D. thesis, Utah University (unpublished).

[27]J. A. Riddick and W. B. Bunger, *Organic Solvent: Physical Properties and Methods of Purification* (Wiley, New York, 1970).

[28]B. Themans, W. R. Salaneck, and J. L. Bredas, Synth. Met. **28**, C359 (1989).